

COBEM2023-0730

INFLUENCE OF WORKING FLUID ON MICRO-PIN FIN HEAT SINKS UNDER SINGLE-PHASE FLOW CONDITIONS

Ariany Pereira Moreira

Bruno Alves de Andrade

UNESP - Faculdade de Engenharia de Ilha Solteira, Ilha Solteira - SP, 15385-000

ariany.moreira@unesp.br

bruno.a.andrade@unesp.br

Jéssica Martha Nunes

UNOESTE - Universidade do Oeste Paulista, Faculdade de Engenharia de Presidente Prudente, Presidente Prudente - SP, 19050-920

jessicanunes@unoeste.br

Sushanta K. Mitra

Micro & Nano-Scale Transport Laboratory, Waterloo Institute for Nanotechnology, Department of Mechanical and Mechatronics Engineering, University of Waterloo, Waterloo, Ontario, Canada

skmitra@uwaterloo.ca

Elaine Maria Cardoso

UNESP - Faculdade de Engenharia de São João da Boa Vista, São João da Boa Vista - SP, 13876-750

elaine.cardoso@unesp.br

Abstract. *Micro-pin fins have been used in thermal management systems due to their ability to improve the heat transfer coefficient. The effectiveness of micro-pin fins heat sinks can be affected by factors such as the size and shape of the pins, the spacing between the pins, and the flow rate and fluid properties. Optimizing these parameters is important to ensure the best micro-pin fin performance in many applications, such as microelectronics, energy conversion, and aerospace engineering. Therefore, this work aims to analyze the influence of two different working fluids, HFE-1000 and DI water, on micro-pin fin heat sinks under single-phase flow conditions. The working fluid flows across staggered diamond-shaped pin fins. Square micro pin fins, with 300 μm width, 350 μm height and 250 μm inter-fin space, were manufactured on a copper substrate using the micro-milling process. The single-phase flow tests were performed at different mass fluxes, and the hydrodynamic effects (pressure drop) and thermal performance were investigated. The results showed that the working fluid properties affect flow behavior and pressure drop. Even with the highest pressure drop, the heat transfer coefficient is improved for DI water, which may be due to the higher thermophysical properties compared to the HFE-7100. Such heat transfer gain compensates the increase in the flow resistance.*

Keywords: *micro-pin fins, heat transfer coefficient, pressure drop, deionized water.*

1. INTRODUCTION

It is known that a large amount of heat can cause inefficiency and overload a system, thereby hindering its satisfactory performance. Heat exchangers are used to transfer thermal energy between fluids, solids, or surfaces (KREITH and BOHN, 2003).

Tuckerman and Pease (1981) are widely recognized as pioneers in developing microchannel heat sinks. The relationship between volume and contact surface area increases with the reduction of the hydraulic diameter of the channel, thus reducing the material for manufacturing and the volume of refrigerant fluid (AHMED et al., 2018). With the progress in research on cooling systems based on microchannels for heat dissipation, specialists began recognizing the restrictions associated with using this specific configuration during the convective boiling process. It was found that implementing microchannels brings significant benefits in terms of Heat Transfer Coefficient (HTC), especially when the coolant is introduced into the system at a subcooled temperature. However, as the vapor quality increases along the microchannels, the flow pattern changes, resulting in thermal instabilities that negatively impact the overall heat transfer performance (KADAM and KUMAR, 2014; KANDLIKAR, 2016).

Using micro-pin fins, Ma et al. (2022) conducted comparative experiments using deionized water to investigate flow boiling instability and pressure drop characteristics. The authors reported an increase in the HTC of up to 150%; according to the authors, micro-pin fins promote capillary pressure by increasing the rewetting of the heated surface; that is, more liquid is directed to hotspots (dry and high-temperature regions) due to capillary force, leading to a

decrease in surface temperature. Qin et al. (2021) conducted comparative experiments between different micro-pin fin shapes during convective boiling. Compared to circular, elliptical, and triangular shapes, the diamond shape showed the most significant increase in HTC due to its ability to separate and migrate vapor film and bubbles.

The pin fin geometry depends on the specific fluid properties and application requirements. The geometry of the micro-pin fins can significantly impact the heat transfer coefficient and pressure drop (JUNG et al., 2021). Firstly, the increased surface area of micro-pin fins means more surface available for heat transfer (this increased surface area results in a higher overall heat transfer coefficient). Second, the presence of fins can also generate vortices and turbulence in the fluid flowing over them. This turbulence enhances the mixing of the fluid and increases the convective heat transfer coefficient, leading to improved heat transfer performance.

Concerning the fluid properties, the prime candidates for immersion cooling the dielectric liquids, unfortunately, possess substantially different thermophysical properties than those of water; for boiling, the poor thermophysical properties and very low surface tension make the dielectrics fluids require very high wall superheats for boiling initiation.

Micro-pin fins have been shown to improve thermal performance by increasing the surface area and inducing turbulence (NUNES et al., 2023). However, the impact of working fluid on single-phase flow, which affects the system's overall performance, is not well understood. Therefore, there is a need to investigate the influence of fluid properties on single-phase flow to optimize their design for specific applications. Understanding the effect of different working fluids on flow behavior and pressure drop can help improve the performance and efficiency of various engineering systems, thereby reducing energy consumption and environmental impact. Hence, the current study investigates heat transfer and pressure drop performance in a micro-pin fin heat sink with different working fluids. The current work can help develop more efficient and optimized microscale thermal management systems to meet the increasing demand for miniaturized devices and systems.

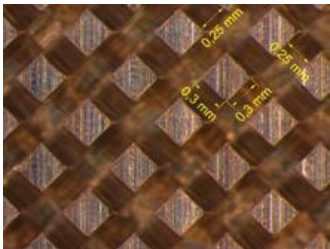
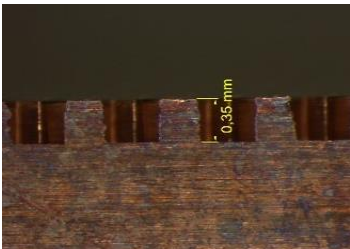
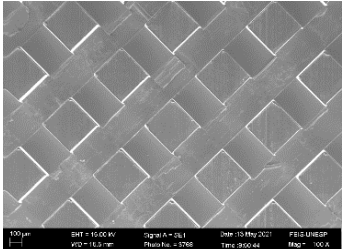
2. MATERIALS AND METHODS

The square micro-pin fins were manufactured on a copper surface (20 x 15 mm), using the micro-milling process, with 350 μm height, 300 μm width, and 250 μm of inter-fin spacing. Figure 1 shows top-view images of the staggered diamond-shaped pin fins analyzed in the current work. Moreover, Table 1 shows the geometric characterization of the micro-pin fin heat sink, which consists of 988 micro-pin fins.



Figure 1 - Image (top view) of the heat sink with staggered diamond-shaped pin fins.

Table 1 - Structural characterization of the micro-pin fin heat sink. (Nunes et al., 2023).

Surface	STEREO			SEM (100x)
	Top view	Side view		
Staggered				

Five K-type thermocouples are embedded in the heat sink to determine the wall temperature and verify the one-dimensional heat conduction along the copper block (Figure 2a). The wall temperature was determined by extrapolating the linear temperature profile, with an R-square error of approximately 1.0 for all heat flux values.

An electrical cartridge resistance with 250 W/220 V, powered by a power source, provides the necessary power. A polycarbonate plate covering the heat sink allows the flow visualization (using a high-speed camera Photron SA3 model with 1000 fps and 1024x1024 resolution). The test section's thermal insulation is made using a ceramic and a polytetrafluoroethylene piece (Figure 2b), in which the inlet and outlet plenums of the heat sink were manufactured with dimensions of 10 x 15 x 10 mm (height x width x length); K-type thermocouples measure the inlet and outlet fluid temperatures. Channels with 0.75 mm depth were manufactured between the plenums and the heat sink to minimize flow entrance turbulence.

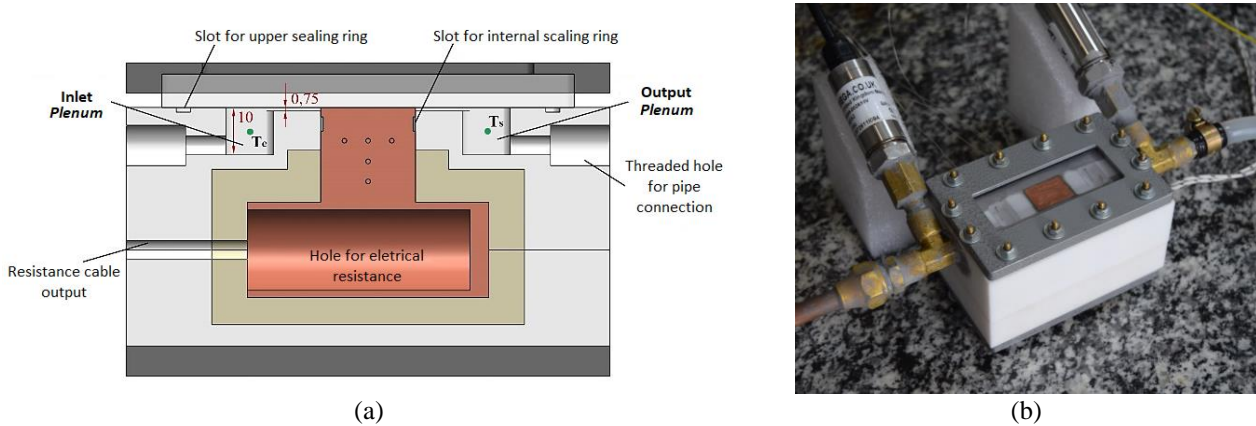


Figure 2 - Micro-pin fin heat sink. (a) Front view of the design (measurements in mm) (Nunes et al., 2023); (b) Photo from test section.

Figure 3 shows the experimental setup used in the current study. A gear pump, controlled by a frequency inverter, was used to displace the fluid (DI water) from the reservoir. A Coriolis mass flow meter (Yokogawa ROTAMASS Total Insight with 0.2% mass flow accuracy) was installed upstream of the preheater, which consists of a copper tube heated by an electrical tape resistance. The working fluid flows through the preheater, ensuring it enters the test section at pre-established temperature conditions. At the inlet and outlet of the preheater, thermocouples and pressure transducers allow the temperature and pressure measurement, respectively. In the test section, two absolute pressure transducers (Omega model PXM309) measure the inlet and outlet pressures, and K-type thermocouples measure the inlet and outlet fluid temperatures. A condenser is installed downstream of the test section to reduce the enthalpy of the working fluid, returning it to its liquid state before returning to the reservoir.

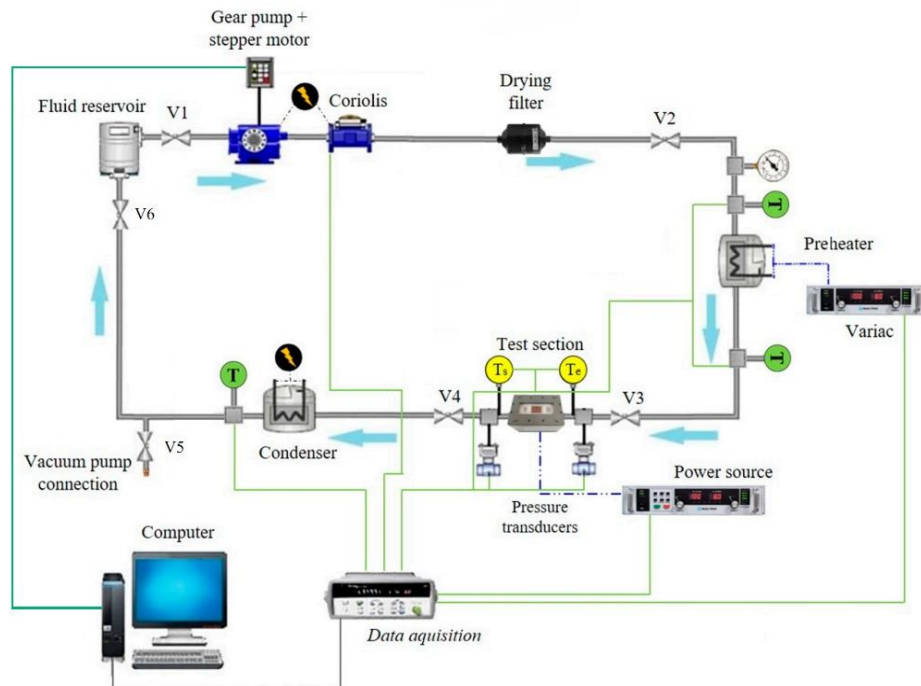


Figure 3 - Schematic diagram of the experimental apparatus (adapted from Nunes et al., 2023).

The tests were performed for different mass fluxes and footprint heat flux of 40 kW/m² (corresponding to an input power of 12 W). The gear pump's rotation was set to achieve the desired mass flux; the preheater was adjusted until its outlet temperature was equal to the desired inlet temperature at the test section (approximately 22 °C). The data were recorded by a data acquisition system (Agilent 34970A) every 2 s after achieving the steady-state regime, characterized by temperature variations lower than the thermocouples uncertainties (± 0.3 °C). The pressure, temperatures, mass flux, and electrical voltage were constantly monitored. The same procedure was adopted during all the experimental tests to ensure repeatability. In order to calculate the heat flux and heat transfer uncertainties, the method described by Kline and McClintock (1953) was used; the uncertainty of the heat flux and the heat transfer coefficient varied from 6 to 15 % and from 13 to 21 %, respectively.

2.1 Data reduction

Equations (1) to (4) are used to calculate the experimental heat transfer coefficient, h_{eff} [W/m² °C], based on Prajapati et al. (2017) and similar studies.

$$Q_{\text{loss}} = Q_{\text{in}} \cdot \dot{m} \cdot c_p \cdot \Delta T \quad (1)$$

where \dot{m} corresponds to the mass flow rate [kg/s], c_p to the specific heat capacity [J/kg·K], and ΔT the difference between the fluid temperature at the inlet and outlet. All analyses consider the effective heat flux, calculated by subtracting the heat loss to the surroundings from the supplied power. In the present study, the heat loss (Q_{loss}) varied from 13 to 35% over varying parameters.

The effective heat flux, q''_{eff} [kW/m²], based on the total surface area in contact with the working fluid (A_t), is calculated by:

$$q''_{\text{eff}} = \frac{(Q_{\text{in}} - Q_{\text{loss}})}{A_t} \quad (2)$$

where,

$$A_t = (A_p - N \cdot A_c) + \eta \cdot N \cdot P_{\text{ma}} \cdot H \quad (3)$$

where A_p corresponds to the footprint area of the heating surface, A_c is the cross-sectional area of the micro-pin fin, N is the total number of micro-pin fins, η is the pin fin efficiency, P_{ma} is the pin fin perimeter, and H is the height of the micro-pin fins.

Therefore, the effective heat transfer coefficient can be calculated by:

$$h_{\text{eff}} = \frac{q''_{\text{eff}}}{T_w - T_f} \quad (4)$$

where T_w is the average temperature of the heat sink provided by three K-type thermocouples fixed within the heat sink surface, and T_f is the average temperature of the working fluid, given by the arithmetic mean between the inlet and outlet fluid temperature. The pressure drop through the test section is given by the difference between the values measured by the transducers (OMEGA PX309 model, with 0.25% accuracy) at the inlet and outlet of the test section, plus the pressure drop due to contraction and expansion obtained by the method described in Chalfi and Ghiaasiaan (2008).

3. EXPERIMENTAL RESULTS AND DISCUSSION

As shown in Figure 4 (for a footprint heat flux of 40 kW/m²), the DI water flowing through the staggered diamond-shaped pin fins resulted in the highest pressure drop, which may not be desirable in some applications. Higher viscosity fluids result in higher resistance to flow, leading to a higher pressure drop compared to the HFE-7100. Moreover, the fluid density affects the fluid's momentum and flow rate through the micro-pin fins; higher-density fluids require more force to be pumped through the system, resulting in increased pressure drop.

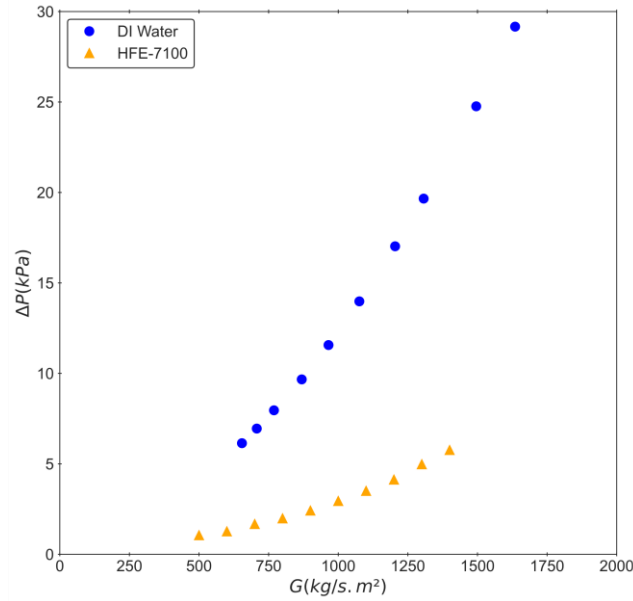


Figure 4 - Effect of fluid properties on micro-pin fins under single-phase flow.

Figure 5 compares the heat transfer performance for different working fluids and mass fluxes, for a 40 kW/m² footprint heat flux. The DI water yields a higher thermal performance at a similar flow rate because of higher thermal conductivity and specific heat capacity, allowing better heat transfer and enhancing the cooling performance. Similarly, Nakayama (1999) highlighted the superiority of water cooling, especially in microscale flows.

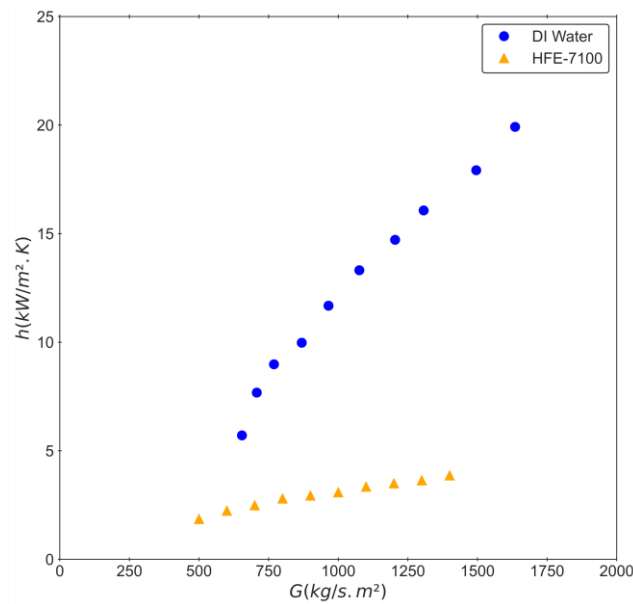


Figure 5 - HTC behavior for deionized water and HFE-7100 on micro-pin fins under single-phase flow.

Generally, the thermal performance index (TPI), similar to that introduced by Mohammadi and Koşar (2017), is used to analyze the thermal benefits of a system relative to the pressure drop penalty. In the current work, TPI is defined as

$$TPI = \frac{h_{water}}{h_{HFE-7100}} \left(\frac{\Delta p_{water}}{\Delta p_{HFE-7100}} \right)^{1/3} \quad (5)$$

i.e., the ratio of the non-dimensionalized heat transfer coefficient to the non-dimensionalized pressure drop.

The existing synergy between the Nusselt coefficients and the pressure drop was applied in order to broadly evaluate the hydrothermal behavior of the channel characterized by an undulating geometry. This examination was conducted using the Heat Transfer Interface (TFI) concept. This analysis used HTC for both deionized water and HFE-7100, along with the corresponding pressure losses. These two aspects' discrepancies stem from the working fluids' different properties.

Despite the increased pressure drop penalty, TPI for DI water was higher for all mass fluxes tested (approximately $TPI = 4$). $TPI > 1$ means the heat transfer coefficient and pressure loss for deionized water are greater than those for HFE-7100, and the TPI for DI water performs better (the HTC enhancement overcomes the pressure-drop penalty).

The experimental pressure drop and Nusselt number results for DI-water were compared with correlations from Liu et al. (2011). Their work investigated the pressure drop and heat transfer in staggered micro square high pin fins using deionized water as the working fluid. In order to predict the characteristics of flow friction, two correlations are proposed, depending on the Reynolds number based on the minimum channel width:

$$f = 1.6361Re_c^{-0.01076}E^{-0.94496} \quad (6)$$

where $E = \frac{2S_t}{w_c/\sin(45^\circ)}$, in which S_t is the transverse pitch, and w_c is the width of the channel. For pressure drop, the following Equation is used:

$$\Delta P_{Liu \text{ et al.}} = N_L \cdot f \left(\frac{G^2}{2\rho} \right) \quad (7)$$

where N_L is the row number of pin fins in the flow direction.

Similarly, for heat transfer performance, Liu et al. (2011) proposed a correlation based on classic heat transfer theory, in which the Nu number is a function of the Reynolds number and the Prandtl number, as shown in Equation (8).

$$Nu_{Liu \text{ et al.}} = 0.1245 Re^{0.6106} Pr_f^{0.36} \left(\frac{Pr_f}{Pr_w} \right)^{0.25} \quad (8)$$

where Pr_f is the Prandtl number at average water bulk temperature, and Pr_w is the Prandtl number at average micro-pin fin base temperature.

The mean absolute error (MAE) for pressure drop was, on average, 29%, related to Liu et al. (2011). For the Nusselt number, Liu et al. (2011) correlation best fit the experimental data, with an average MAE of 14.1%. The deviation observed between the previous correlation and the current data is not necessarily related to the weaknesses of the correlation but may be to the geometric parameters and operating conditions since the prediction performance could be related to the property of the fluid (even though the Prandtl number implies a more general application, it does not guarantee the general application of these correlations) and the geometric configuration, since the size, shape and spacing between the pins affect the overall system performance — for example, Liu et al. (2011) based their correlations on a database for square micro-pin fins heat sinks with an array of 625 pin fins with 3 mm height.

4. CONCLUSIONS

This study investigated the hydrodynamic and thermal behavior of DI water single-phase flow compared to HFE-7100 in an array of staggered square micro-pin-fins. The working fluid HFE-7100 showed better results in terms of pressure drop compared to deionized water. This difference is mainly attributed to the viscosity of the fluids used. The viscosity of deionized water is higher than that of HFE-7100, leading to increased frictional losses and higher pressure drop. Furthermore, deionized water exhibits high thermal conductivity in heat transfer and a greater capacity to absorb and store heat due to its higher specific heat capacity than HFE-7100. The differences in the physicochemical properties between deionized water and HFE-7100, such as viscosity, polarity, thermal conductivity, and specific heat capacity, significantly influence the flow behavior and heat transfer.

The experimental results for DI water were compared with Liu et al. (2011) correlation developed for the same micro-pin fin shape and arrangement. For pressure drop and Nusselt number, a mean absolute error (MAE) of 29% and 14.1% were found, respectively.

Therefore, not only the geometrical parameters of the micro-pin fins but also the fluid properties should be considered in order to optimize the design of a microheat sink. Even with a higher pressure-drop penalty, the system's performance is better for DI water since the TPI is higher than 1 (the HTC improvement overcomes the highest pressure

drop). Concerning the improvement of prediction methods, more studies are required for different combinations of engineered surfaces and working fluids, considering their thermophysical properties, morphological features of the heated surfaces, and flow testing conditions.

In this way, a more detailed quantitative study is underway to analyze the HTC and pressure drop under convective flow boiling to understand better the physical phenomena and their influences on the system's performance.

5. ACKNOWLEDGEMENTS

The authors would like to thank UNESP for the financial support provided by PPGEM – UNESP/FEIS, CAPES (88887.677996/2022-00), CNPq (458702/2014-5 and 309848/2020-2) and FAPESP (2013/15431-7, 2019/02566-8 and 2022/03946-1). The authors also thank Prof. Alessandro Roger Rodrigues from Escola de Engenharia de São Carlos/USP and Prof. Ricardo Arai from IFSP/São Carlos for their important contributions to this work.

6. REFERENCES

- AHMED, H. E.; SALMAN, B.H.; KHERBEET, A. S.; AHMED, M. I. "Optimization of thermal design of heat sinks: A review". *International Journal of Heat and Mass Transfer*, v. 118, p. 129-153, 2018.
- CHALFI, T.Y.; GHIAASIAAN, S. "Pressure drop caused by flow area changes in capillaries under low flow conditions". *International Journal of Multiphase Flow*, v. 34(1), p. 2 – 12, 2008.
- JUNG, D.; LEE, H.; KONG, D.; CHO, E.; JUNG, K.W.; KHARANGATE, C.R.; IYENGAR, M.; MALONE, C.; ASHEGHI, M.; GOODSON, K.E. "Thermal design and management of micro-pin fin heat sinks for energy-efficient three-dimensional stacked integrated circuits." *International Journal Of Heat And Mass Transfer*, v. 175, p. 121192, 2021.
- KADAM, S. T.; KUMAR, R. "Twenty-first-century cooling solution: microchannel heat sinks." *International Journal of Thermal Sciences*, vol. 85, p. 73-92, 2014.
- KANDLIKAR, S. G. "Mechanistic considerations for enhancing flow boiling heat transfer in microchannels." *Journal of Heat Transfer, ASME*, vol. 138(2), 021504, 2016.
- KLINE, S.J.; MCCLINTOCK, F.A. "Describing uncertainties in single sample experiments", *Mechanical Engineering*, 75, p. 3 – 8, 1953.
- KREITH, F.; BOHN, M.S. *Princípios de transferência de calor*. Trad. All Tasks, Pioneira Thomson Learning. São Paulo, 2003.
- LIU, M.; LIU, D.; XU, S.; CHEN, Y. "Experimental study on liquid flow and heat transfer in micro square pin fin heat sink". *International Journal of Heat and Mass Transfer*, vol. 54, p. 5602–5611, 2011.
- MA, X.; JI, X.; WANG, J.; YANG, X.; ZHANG, Y.; WEI, J. "Flow boiling instability and pressure drop characteristics based on micro-pin-finned surfaces in a microchannel heat sink". *International Journal of Heat and Mass Transfer*, [S.L.], v. 195, p. 123168, 2022.
- MOHAMMADI, A., AND KOŞAR, A. "Hydrodynamic and Thermal Performance of Microchannels with Different Staggered Arrangements of Cylindrical Micro Pin Fins." ASME. *Journal of Heat Transfer*, vol. 139(6): 062402, 2017.
- NAKAYAMA, W. "Enhanced Heat Transfer in Tight Space — A Frontier for Thermal Management of Microelectronic Equipment." *In Enhanced Heat Transfer*, p. 121–133, 1999.
- NUNES, J. M.; OLIVEIRA, J. D.; COPETTI, J. B.; GAJGHATE, S. S.; BANERJEE, U.; MITRA, S. K.; CARDOSO, E. M. "Thermal Performance Analysis of Micro Pin Fin Heat Sinks under Different Flow Conditions". *Energies*, [S.L.], v. 16, n. 7, p. 3175, 2023.
- PRAJAPATI, Y. K.; PATHAK, M.; KHAN, M. K. "Bubble dynamics and flow boiling characteristics in three different microchannel configurations." *International Journal of Thermal Sciences*, vol. 112, p. 371-382, 2017.
- QIN, L.; LI, S.; ZHAO, X.; ZHANG, X.. "Experimental research on flow boiling characteristics of micro pin-fin arrays with different hydrophobic coatings". *International Communications In Heat And Mass Transfer*, [S.L.], v. 126, p. 105456, 2021.
- TUCKERMAN, D.B.; PEASE, R.F.W." High-performance heat sinking for VLSI". *Ieee Electron Device Letters*, [S.L.], v. 2, n. 5, p. 126-129, 1981.

7. RESPONSIBILITY NOTICE

The authors are the only ones responsible for the printed material included in this paper.